Unraveling the Origin of Regioselectivity in Rhodium Diphosphine Catalyzed Hydroformylation. A DFT QM/MM Study

Jorge J. Carbó,[†] Feliu Maseras,[†] Carles Bo,*[,‡] and Piet W. N. M. van Leeuwen[§]

Contribution from the Unitat de Química Física, Edifi C.n, Universitat Autònoma de Barcelona, 08193 Bellaterra, Barcelona, Spain, Departament de Química Física i Inorgànica and Institut d'Estudis Avançats, Universitat Rovira i Virgili, Pl. Imperial Tarraco, 1, 43005 Tarragona, Spain, and Institute for Molecular Chemistry, University of Amsterdam, Nieuwe Achtergracht 166, 1018 WV Amsterdam, The Netherlands

Received January 22, 2001

Abstract: The origin of regioselectivity in rhodium diphosphine catalyzed hydroformilation was investigated by means of hybrid QM/MM calculations using the IMOMM method. The roles of the diphosphine bite angle and of the nonbonding interactions were analyzed in detail by considering rhodium systems containing xantphos-type ligands, for which a correlation between the natural bite angle and regioselectivity has been recently reported. From the pentacoordinated equatorial−equatorial HRh(CO)(alkene)(diphosphine) key intermediate, eight possible reaction paths were defined and characterized through their respective transition states (TS). We succeeded in reproducing the experimentally observed trends for the studied diphosphines. By performing additional calculations on model systems, in which the steric effects induced by the phenyl substituents of xantphos ligands were canceled, we were able to separate, identify, and evaluate the different contributions to regioselectivity. These additional calculations showed that regioselectivity is governed by the *nonbonding* interactions between the diphenylphosphino substituents and the substrate, whereas the effects directly associated to the bite angle, what we call *orbital effects*, seem to have a smaller influence.

Introduction

Rhodium-catalyzed hydroformylation is one of the most prominent applications of homogeneous catalysis in industry.[1] Extensive research has been devoted to the development of new ligands with different stereoelectronic properties, pursuing better activities and regio- and stereoselectivities. Among several types of ligand-modified catalysts, those containing phosphines and phosphites have exhibited the highest activity and selectivity in the hydroformylation of terminal alkenes. Systematic studies of the influence of ligand structure on catalytic performance in the hydroformylation reaction are rare, and despite the development of a wide variety of ligands, consistent structure−activity relationships are still lacking. The reason for this is that *a complex web of electronic and steric effects governs selectivity in hydroformylation.*[2] The term *electronic effect* accounts for the electronic properties of ligands (basicity, π acceptor/donor capabilities) whereas steric effects refer to ligand bulkiness. Diphosphine ligands generate two kinds of steric effects: those originated by ligand−ligand or ligand−substrate nonbonding interactions (*nonbonding effects*) and those directly related to the bite angle, which we will call *orbital effects*. The bite angle determines metal hybridization and this in turn metal orbital energies, therefore those steric effects are in fact electronic effects. The situation becomes still more complicated because the bite angle also affects ligand bulkiness.

Few studies have paid attention to the electronic properties of phosphine ligands and their influence on catalytic performance.[3] These studies showed that less basic phosphines afford higher activity and higher linear over branched (l:b) ratios. Casey and co-workers[4] demonstrated a different effect on the l:b ratio when electronically modified asymmetric diphosphines occupy apical or equatorial positions. Using a series of xantphos ligands,[5] which ensured a strict cancellation of nonbonding and orbital effects, Van der Veen et al.[6] proved that the l:b ratio and the activity increase with decreasing phosphine basicity and that the l:b ratio is, within the narrow range of ligands studied, independent of the chelation mode of the diphosphine.

Diphosphine steric effects have been rationalized with the help of the natural bite angle concept introduced by Casey and Whiteker[7] as a characteristic of a chelate ligand. The influence of natural bite angles on the activity and regioselectivity has been observed for several catalytic reactions.[5,8,9] However, it is

[†] Universitat Autònoma de Barcelona.
[‡] Universitat Rovira i Virgili.
[§] University of Amsterdam.

(1) See for instance: van Leeuwen, P. W. N. M.; van Koten, G. In *Catalysis: an integrated approach to homogeneous, heterogeneous and industrial catalysis*; Moulijn, J. A., van Leeuwen, P. W. N. M., van Santen, R. A., Eds.; Elsevier: Amsterdam, The Netherlands, 1993; pp 201−202. Beller, M.; Cornils, B.; Frohning, C. D.; Kohlpaintner, C. W. *J. Mol. Catal. A: Chem.* **1995**, *104*, 17−85. Frohning, C. D.; Kohlpaintner, C. W. In *Applied Homogeneous Catalysis with Organometallic Compounds: a comprehensive handbook in two volumes*; Cornils, B., Herrman, W. A., Eds.; VCH: Weinheim, 1996; Vol. 1, pp 27−104.

(2) Casey, C. P.; Paulsen, E. L.; Beuttenmueller, E. W.; Proft, B. R.; Petrovich, L. M.; Matter, B. A.; Powell, D. R. *J. Am. Chem. Soc.* **1997**, *119*, 11817.

(3) (a) Moser, W. R.; Papile, C. J.; Brannon, D. A.; Duwell, R. A.; Weininger, S. J. *J. Mol. Catal.* **1987**, *41*, 271−292. (b) Unruh, J. D.; Christenson, J. R. *J. Mol. Catal.* **1982**, *14*, 19.

(4) Casey, C. P.; Paulsen, E. L.; Beuttenmueller, E. W.; Proft, B. R.; Matter, B. A.; Powell, D. R. *J. Am. Chem. Soc.* **1999**, *121*, 63.

(5) Kranenburg, M.; van der Burgt, Y. E. M.; Kamer, P. C. J.; van Leeuwen, P. W. N. M. *Organometallics* **1995**, *14*, 3081.

(6) van der Veen, L. A.; Boele, M. D. K.; Bregman, F. R.; Kamer, P. C. J.; van Leeuwen, P. W. N. M.; Kees, G.; Fraanje, J.; Schenck, H.; Bo, C. *J. Am. Chem. Soc.* **1998**, *120*, 11616.

(7) Casey, C. P.; Whiteker, G. T. *Isr. J. Chem.* **1990**, *30*, 299.

10.1021/ja0101678 CCC: $20.00
Published on Web 07/17/2001

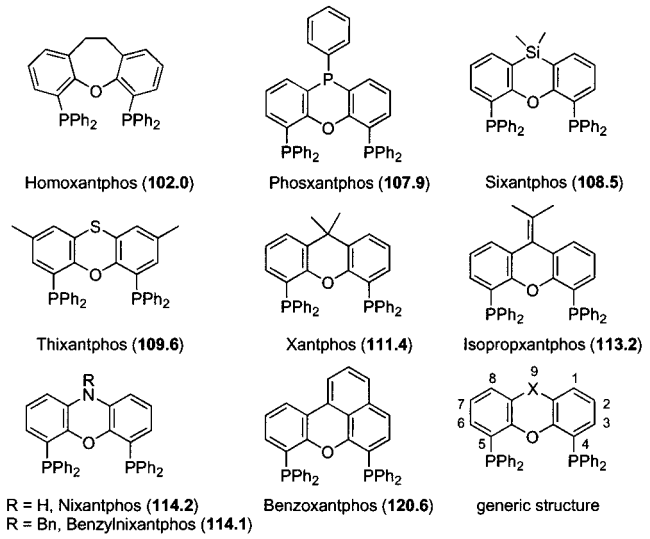

Figure 1. Schematic representation of the xantphos ligand family. The natural bite angle is given in parentheses.

still not understood in detail how the bite angle affects the regioselectivity. Very recently, a series of xantphos-type ligands (see Figure 1) with natural bite angles ranging from 102 to 121° were synthesized, and the effect of the natural bite angle on coordination chemistry and catalytic performance was studied.[9] Xantphos ligands in Figure 1 have been especially designed to ensure that mutual variation in electronic properties and in steric size within the series is minimal and that the bite angle is the only characteristic that has a significant variation within the series. In the hydroformylation of 1-octene an increase in selectivity for linear aldehyde formation and activity was observed with increasing natural bite angle. For styrene the same trend in selectivity for the linear aldehyde was found, although for that substrate selectivity was also found to be dependent on temperature and CO pressure. These findings suggest that the bite angle affects the selectivity in the steps of alkene coordination and hydride migration (or alkene insertion). A plausible explanation of the bite angle effect is that when the natural bite angle increases, the congestion around the metal atom also increases, which in turn favors the less steric demanding transition state (TS), that is, the TS that drives the reaction toward linear product. This hypothesis has given impetus to the realization of the work presented here, aiming to provide a quantitative answer to such a question.

The fundamental catalytic steps for rhodium hydroformylation with PPh_3 as proposed by Wilkinson[10] are shown in Scheme 1. According to this generally accepted mechanism, the selectivity for linear or branched product is determined in the alkene insertion step, provided that this is irreversible. Thus, the alkene complex can lead either to linear or to branched Rh−alkyl complexes, which, in the subsequent catalytic steps, will generate linear and branched aldehydes, respectively. Several theoretical studies have been performed in the elementary alkene insertion step, using ethene as a model for alkene and PH_3 as a model for phosphines.[11] Very recently, Rocha and de Almeida[12] have used propene instead of ethene as the substrate to

Scheme 1

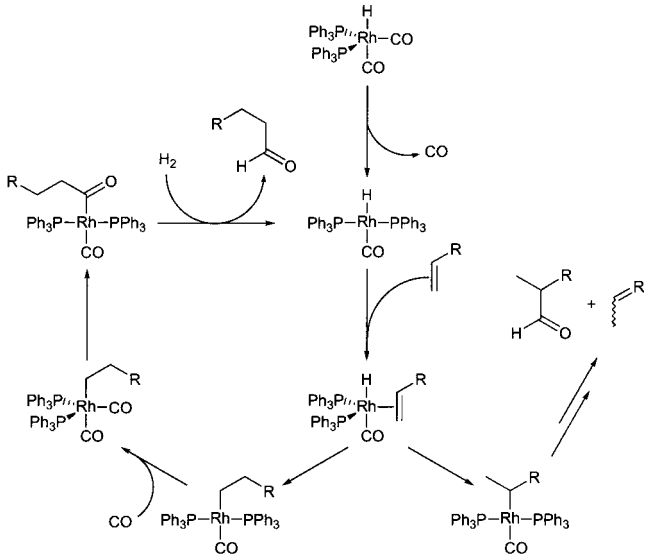

investigate the regioselectivity in the hydroformylation reaction. Using $HRh(CO)(PH_3)_2$ as a model for catalytic species, those authors observed a preference for the reaction to take place at the terminal alkene carbon, which favors the yield of linear aldehyde. Morokuma and co-workers[13] have studied the whole hydroformylation cycle of modified rhodium complexes, employing a model system using phosphines (PH_3) and ethene as substrate. However, the use of PH_3 as a model of phosphine ligands is a drastic simplification, and this is obviously not so good as far as ligand interactions are concerned. The significance of theoretical studies using model systems for understanding catalytic processes has been reported in several reviews.[14] Besides that, nowadays, most of the research effort in catalysis is made in developing new ligands with tailor stereoelectronic properties. Thus, more elaborate computational models, mimicking as much as possible the structure of the catalyst, would be desirable for understanding the effects of diphosphine ligands on reactivity.

Herrmann and co-workers[15] made a first contribution to the theoretical description of systems tested experimentally using a combined quantum mechanics/molecular mechanics (QM/MM) approach. They investigated the regioselectivity of propene on Rh-catalyzed hydroformylation. The method used consists of a full QM treatment of a model system (i.e. with PH_3) and a subsequent addition of phosphine substituents, which are described by MM, substituting the H atoms of PH_3 but keeping frozen the atoms already described in the QM region. This kind of approach has some limitations due to the lack of relaxation of reactive centers (in the QM region) under the influence of the ligands. Thus, despite the relaxation of the ligands upon complexation, the steric strain induced by the ligands on reactive centers cannot be assessed, and properties such as relative energies of transition states, which depend on diphosphine

(8) (a) Casey, C. P.; Whiteker, G. T.; Melville, M. G.; Petrovich, L. M.; Gavney, J. A., Jr.; Powell, D. R. *J. Am. Chem. Soc.* **1992**, *114*, 5535. (b) Kranenburg, M.; Kamer, P. C. J.; van Leeuwen, P. W. N. M. *Eur. J. Inorg. Chem.* **1998**, 25.

(9) van der Veen, L. A.; Keeven, P. H.; Schoemaker, G. C.; Reek, J. N. H.; Kamer, P. C. J.; van Leeuwen, P. W. N. M.; Lutz, M.; Spek, A. L. *Organometallics* **2000**, *19*, 872.

(10) Evans, D.; Osborn, J. A.; Wilkinson, G. *J. Chem. Soc. (A)* **1968**, 3133.

(11) (a) Thorn, D. L.; Hoffmann, R. *J. Am. Chem. Soc.* **1978**, *100*, 2079. (b) Koga, N.; Jin, S. Q.; Morokuma, K. *J. Am. Chem. Soc.* **1988**, *110*, 3417. (c) Siegbahn, P. E. M. *J. Am. Chem. Soc.* **1993**, *115*, 5803.

(12) Rocha, W. R.; de Almeida, W. B. *Int. J. Quantum Chem.* **2000**, *78*, 42.

(13) Matsubara, T.; Koga, N.; Ding, Y.; Musaev, D. G.; Morokuma, K. *Organometallics* **1997**, *16*, 1065.

(14) (a) Koga, N.; Morokuma, K. *Chem. Rev.* **1991**, *91*, 823. (b) Musaev, D. G.; Morokuma, K. *Adv. Chem. Phys.* **1996**, *45*, 61. (c) Niu, S.; Hall, M. B. *Chem. Rev.* **2000**, *100*, 353. (d) Torrent, M.; Sola, M.; Frenking, G. *Chem. Rev.* **2000**, *100*, 439.

(15) Gleich, D.; Schmid, R.; Herrmann, W. A. *Organometallics* **1998**, *17*, 4828.

structure, cannot be properly computed. Also pure MM methods have been employed by other authors to investigate ligand−substrate interactions in intermediates of the hydroformylation process and their influence on regioselectivity.[16]

In this paper we report a theoretical study based on the first principles IMOMM method[17] on Rh−diphosphine catalyzed hydroformylation. Our goal is to provide a quantitative theoretical characterization of the origin of regioselectivity in Rh−diphosphine systems, focusing the study on the experimentally characterized xantphos systems, for which variation in electronic properties is minimal. Furthermore, the use of the IMOMM method, which only accounts for the steric properties of ligands, is fully justified. Thus, we seek to evaluate the effect of the bite angle on regioselectivity, as well as to gain knowledge about the counterbalance of *nonbonding* and *orbital effects*. Unlike previous studies, this study has been carried out with a method such as IMOMM, which allows the full optimization of minima and transition states.

We will focus our study on two diphosphine ligands, benzoxantphos and homoxantphos, which represent the extreme cases of natural bite angle among the series of xantphos ligands. We will use propene as a model for terminal aliphatic alkenes. Since the alkene insertion is the crucial step, we first explore in detail its mechanism using ethene as a model for the alkene. The relative energies of the transition states corresponding to the propene insertion will be used to predict the regioselectivity. Finally, we will analyze the effects that govern regioselectivity by performing additional calculations in a new model system, in which the steric effects induced by the phenyl substituents of xantphos ligands are canceled.

Computational Details

Hybrid QM/MM calculations with the IMOMM method[17] were carried out with a program built from modified versions of the two standard programs: Gaussian 92/DFT[18] for quantum mechanics part and MM3(92)[19] for the molecular mechanics part. The QM region of the catalyst was $RhH(CO)(PH_3)_2$, while the substrate, ethene or propene, was fully in the QM region. The ab initio calculations were done within the framework of the density functional theory (DFT)[20] using the B3LYP functional.[21] A quasirelativistic effective core potential operator was used to represent the 28 innermost electrons of the Rh atom, as well as the 10 innermost electrons of the P atom.[22] The basis set for Rh and P atoms was that associated with the pseudopotential,[22] with a standard double-ξ LANL2DZ contraction,[18] and in the case of P was supplemented by a d shell.[23] The 6-31G(d) basis set was used for the alkene carbons and the carbonyl ligand,[24] the 6-311G(p) basis set was used for the hydride ligand,[24] whereas the 6-31G basis set was used for the other carbon and hydrogen atoms.[24] Molecular mechanics calculations used the MM3(92) force field.[25] Default parameters were used when available, otherwise those of similar atoms replaced the missing ones. The van der Waals parameters for the rhodium atom were taken from the UFF force field,[26] and torsional contributions involving dihedral angles with the metal atom in terminal position were set to zero. All the geometrical parameters were optimized except for the P−H (1.42 Å) bond distances in the molecular orbital part of IMOMM and the $P-C(sp^2)$ (1.843 Å) distances in the MM part of IMOMM.

Mechanistic Considerations and Assumptions

Free energy profiles recently have been proposed to discuss the kinetics and the reaction mechanism.[27] It is assumed that alkene insertion is irreversible and rapid preequilibria exist for CO and alkene association and dissociation. The rate-determining step can be either CO dissociation or alkene coordination or alkene insertion, all involved intermediates being in equilibrium. However, it is still neither clear[27] if the rate-determining and the selectivity determining steps coincide nor if the selectivity is determined by the HRh(CO)(alkene)(diphosphine) intermediate, never observed experimentally. Previous ab initio calculations in model systems have shown an axial preference of the hydride in related pentacoordinated TBP complexes, with the alkene occupying an equatorial position and oriented parallel to the equatorial plane.[13] Moreover, these studies on alkene insertion have also shown that the most favorable path for this process goes through this kind of intermediate. HPIR measurements[3a,6,28] have shown that the catalyst resting state is precisely a trigonal bipyramid $HRh(CO)_2$(xantphos) complex, which is present in two isomers, labeled according to the position of the phosphine ligands as equatorial−equatorial (**ee**) and equatorial−apical (**ea**). Both isomers are in rapid equilibrium, the **ee** isomer being predominant over the **ea** one. The rate of interconversion is much higher than CO dissociation and hydride migration rates.[2] The alkene complex is obtained from $HRh(CO)_2$(diphosphine) by dissociating one carbonyl molecule. Furthermore, X-ray structures[9] of some HRh(CO)(xantphos)(PPh_3) complexes have shown an **ee** xantphos coordination, containing PPh_3 in the equatorial position and H and CO in the apical ones. Carbonyl dissociation rates for (formyl)$Rh(CO)_2$(phosphite) clearly indicate that the equatorial CO dissociates orders of magnitude faster than the apical carbonyl.[29] These results suggest that the **ee** isomer might be more active than the **ea** one and that alkene could coordinate to the **ee** tetracoordinated resulting complex directly without relaxing to the most stable square-planar complex. The most stable cis should be obtained by a twisting of the H−Rh−CO moiety, which would imply an energy barrier. The flexibility of the xantphos-type ligands allows them to adopt bite angles as large as 164° [30] required for a quasi-trans square-

(16) (a) Castonguay, L. A.; Rappé, A. K.; Casewit, C. J. *J. Am. Chem. Soc.* **1991**, *113*, 7177. (b) Paciello, R.; Siggel, L.; Kneuper, H. J.; Walker, N.; Röper, M. *J. Mol. Catal. A* **1999**, *143*, 85. (c) Casey, C. P.; Petrovich, L. M. *J. Am. Chem. Soc.* **1995**, *117*, 6007.

(17) (a) Maseras, F.; Morokuma, K. *J. Comput. Chem.* **1995**, *16*, 1170. (b) Maseras, F. *Chem. Commun.* **2000**, 1821−1827.

(18) Frisch, M. J.; Trucks, G. W.; Schlegel, H. B.; Gill, P. M. W.; Johnson, B. G.; Wong, M. W.; Foresman, J. B.; Robb, M. A.; Head-Gordon, M.; Replogle, E. S.; Gomperts, R.; Andres, J. L.; Raghavachari, K.; Binkley, J. S.; Gonzalez, C.; Martin, R. L.; Fox, D. J.; Defrees, D. J.; Baker, J.; Stewart, J. J. P.; Pople J. A. *Gaussian 92/DFT*; Gaussian Inc: Pittsburgh, PA, 1993.

(19) Allinger N. L. *MM3(92)*; QCPE: Bloomington IN, 1992.

(20) (a) Parr, R. G.; Yang, W. *Density Functional Theory of Atoms and Molecules*; Oxford University Press: Oxford, U.K., 1989. (b) Ziegler, T. *Chem. Rev.* **1991**, *91*, 651.

(21) (a) Lee, C.; Yang, W.; Parr, R. G. *Phys. Rev. B* **1988**, *37*, 785. (b) Becke, A. D. *J. Chem. Phys.* **1993**, *98*, 5648. (c) Stephens, P. J.; Devlin, F. J.; Chabalowski, C. F.; Frisch, M. J. *J. Phys. Chem.* **1994**, *98*, 11623.

(22) Hay, P. J.; Wadt, W. R. *J. Chem. Phys.* **1985**, *82*, 299.

(23) Höllwarth, A.; Böhme, M.; Dapprich, S.; Ehlers, A. W.; Gobbi, A.; Jonas, V.; Köhler, K. F.; Stegmann, R.; Veldkamp, A.; Frenking, G. *Chem. Phys. Lett.* **1993**, *208*, 237.

(24) (a) Hehre, W. J.; Ditchfield, R.; Pople, J. A. *J. Chem. Phys.* **1972**, *56*, 2257. (b) Hariharan, P. C.; Pople, J. A. *Theor. Chim. Acta* **1973**, *28*, 213. (c) Francl, M. M.; Pietro, W. J.; Hehre, W. J.; Binkley, J. S.; Gordon, M. S.; Defrees, D. J.; Pople, J. A. *J. Chem. Phys.* **1982**, *77*, 3654. (d) McLean, A. D.; Chandler, G. S. *J. Chem. Phys.* **1980**, *72*, 5639. (e) Krishnan, R.; Binkley, J. S.; Seeger, R.; Pople, J. A. *J. Chem. Phys.* **1980**, *72*, 650.

(25) Allinger, N. L.; Yuh, Y. H.; Lii, J. H. *J. Am. Chem. Soc.* **1989**, *111*, 8551.

(26) Rappé, A. K.; Casewit, C. J.; Colwell, K. S.; Goddard, W. A., III; Skiff, W. M. *J. Am. Chem. Soc.* **1992**, *114*, 10024.

(27) van Leeuwen, P. W. N. M.; Casey, C. P.; Whiteker, G. T. In *Rhodium Catalyzed Hydroformylation*; van Leeuwen, P. W. N. M., Claver, C., Eds.; Kluwer-CMC: Dordrecht, The Netherlands, 2000; pp 96−106.

(28) Del Río, I.; Pàmies, O.; van Leeuwen, P. W. N. M.; Claver, C. *J. Organomet. Chem.* **2000**, *608*, 115.

(29) van der Slot, S.-C.; Kamer, P. C. J.; van Leeuwen, P. W. N. M.; Iggo, J. A.; Heaton, B. T. *Organometallics* **2001**, *20*, 430−441.

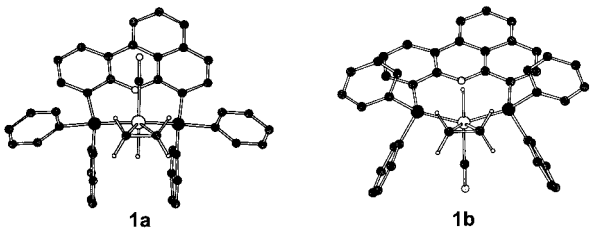

Figure 2. IMOMM structures of HRh(alkene)(CO)(benzoxantphos) isomers **1a** and **1b**. The hydrogen atoms of xantphos ligands are omitted for clarity.

planar structure. Thus, it seems plausible that **ee** equatorial CO dissociation is quickly followed by alkene coordination/insertion.

All above arguments point to the fact that the key intermediate might be the **ee** HRh(CO)(alkene)(xantphos) complex, for which still two isomers can be distinguished depending on the relative hydride and carbonyl positions along the trigonal axis. X-ray structures[9] of some HRh(CO)(xantphos)(PPh_3) show the carbonyl ligand at the same side as the xantphos ligand backbone. We carried out IMOMM calculations on two isomers (**1a** and **1b**) of the pentacoordinate ethene complex HRh(CO)(C_2H_4)-(benzoxantphos) (Figure 2), to check if our computational method was able to reproduce the experimentally reported relative disposition of the hydride and carbonyl axial ligands. In isomer **1a** the carbonyl axial ligand is on the same side of the equatorial plane as the benzoxantphos backbone, while the trans hydride ligand lies between two phenyl moieties on the opposite side. In **1b**, the relative positions of hydride and carbonyl ligands are exchanged. Calculations show that isomer **1a** is more stable than **1b** by 7.5 kJ·mol^{-1}. The accuracy of the computational method to reproduce such small energy differences is obviously questionable, but in any case it is reassuring to be able to reproduce the experimental result. Furthermore, the IMOMM method allows the analysis of the origin of the difference between the two isomers. Decomposition of the energy in QM and MM contributions (see Table 1) shows that differences between **1a** and **1b** are exclusively in the MM part, which clearly indicates a steric origin for the relative stability of the two isomers. The geometry of the predicted most stable isomer, **1a**, is completely consistent with the disposition of axial ligands in X-ray data for the related complex HRh(CO)(PPh_3)(benzoxantphos).[9] In Figure 2, it can be observed how the bulkier CO ligand of isomer **1b** lies between two phenyl moieties, breaking the face-to-face stacking interaction between them and destabilizing the complex. This result illustrates nicely how the IMOMM method is able to transfer nonbonding interactions between QM and MM parts, since what we see in this case is the interaction between the CO (QM part) and the two phenyls (MM part). Stacking interaction has been well-characterized in other chemical systems and its occurrence is therefore not surprising here.[31] Also its importance has been evaluated and characterized using the IMOMM method in previous studies.[32,33] We also examined the existence of other possible conformational isomers of complex **1a**. A new isomer **1a′** was characterized, in which the above-mentioned phenyl moieties present an edge-to-face instead of a face-to-face stacking interaction. Calculations showed that this new conformational isomer is nearly degenerate in energy (Table 1), but it has a different distribution of QM and MM energies.

Let us now focus on the relationship between the structure and activity of the alkene intermediate. A terminal alkene coordinated to the equatorial position of an **ee** HRh(CO)(alkene)-(xantphos) can adopt four different conformations, depending on which face of the double bond coordinates to the metal and on the chain orientation. Figure 3 shows schematically the structure of HRh(CO)(alkene)(xantphos), the alkene being in the front side and the diphosphine backbone behind the metal center. The metal and the carbonyl ligand are omitted for clarity and the labels left/right and up/down are used to name the four conformations, the label indicating the alkene chain orientation. It does not matter, in terms of selectivity, which is the relative stability of these four conformations, since each one can give rise to a pro-linear and to a pro-branched transition state and product. In fact, if a left_up species undergoes a clockwise rotation (CW), the internal carbon inserts into the metal hydride bond, i.e., the terminal carbon is involved in the formation of the new C−H bond and the product is a branched aldehyde labeled as B_in in Figure 3. However, if the same left_up species rotates counterclockwise (CCW), the linear aldehyde L_out will be obtained. Since each conformation generates two products, there are eight possible pathways and consequently eight different transition states. Figure 3 shows the labels used to designate each one, L for linear and B for branched, and in and out to indicate to which direction the chain points: "in" if it points toward the hydride-Rh-carbonyl axis and "out" if it points toward the phosphine phenyl substituents. Thus, we take into account that the regioselectivity is not determined by the structure of the alkene intermediate but by the relative stabilities of all TS's. We consider the use of the TS's energies in the calculation of selectivities a substantial improvement with respect to the use of the energy of intermediates, although we must admit that it is not the optimal solution. The best approach would be the computation of the full catalytic cycle, all intermediates and TS's, from the entry of the substrate to the departure and regeneration of the catalyst, complemented with IRC calculations to confirm the connection between TS's and intermediates. This is, however, out of reach for current computational resources. By using the energy of a particular TS in the calculation of selectivity we are assuming that this TS corresponds indeed to the step where this selectivity is decided. Furthermore, the reaction center of our TS's resembles closely those of previous calculations on propene insertion, for which an IRC calculation was recently performed.[12] Assuming a Boltzmann distribution, the percentage of linear and branched products is easily obtained from the relative energies of all possible TS's. This kind of assumption is the same as the one previously used.[12,15] Most of the reaction paths in Figure 3 have been characterized through the localization of the corresponding TS structure. All transition states located have a negative eigenvalue in the approximate Hessian, and their corresponding normal modes have large values for variables involved in the alkene insertion.

Results and Discussion

1. Ethene Insertion. Before presenting the results for propene, we will first discuss the results for the simplest alkene, ethene. This simplified system will be used to characterize the

(30) (a) Sandee, A. J.; van der Veen, L. A.; Reek, J. N. H.; Kamer, P. C. J.; Lutz, M.; Spek, A. L.; van Leeuwen, P. W. N. M. *Angew. Chem., Int. Ed. Engl.* **1999**, *38*, 3231. (b) van Haaren, R. J.; Goubitz, K.; Fraanje, J.; van Strijdonck, G. P. F.; Oevering, H.; Coussens, B.; Reek, J. N. H.; Kamer, P. C. J.; van Leeuwen, P. W. N. M. *Inorg. Chem.* In press.

(31) (a) Jorgensen, W. L.; Severance, D. L. *J. Am. Chem. Soc.* **1990**, *112*, 4768. (b) Graf, D. D.; Campbell, J. P.; Miller, L. L.; Mann, K. R. *J. Am. Chem. Soc.* **1996**, *118*, 5480. (c) Graf, D. D.; Duan, R. G.; Campbell, J. P.; Miller, L. L.; Mann, K. R. *J. Am. Chem. Soc.* **1997**, *119*, 5888.

(32) Ujaque, G.; Maseras, F.; Lledós, A. *J. Am. Chem. Soc.* **1999**, *121*, 1317.

(33) Vázquez, J.; Pericás, M. A.; Maseras, F.; Lledós, A. *J. Org. Chem.* **2000**, *65*, 7303.

Table 1. Energies and Geometrical Parameters of Reactants and Transition States for Ethene Insertion[a]

	benzoxantphos						homoxantphos		
	1a	**1a′**	**1b**	CW	CCW	CCW[b]	**1a**	CW	CCW
total energy	0.0	0.0	7.5	57.9	58.0	59.2	0.0	64.5	57.5
MM energy	0.0	−3.1	6.7	−2.1	−1.9	−0.1	0.0	4.4	−3.0
QM energy	0.0	3.1	0.7	60.0	59.9	59.2	0.0	60.1	60.6
P−Rh−P	107.4	112.9	120.1	111.4	111.1	106.8	101.8	102.6	99.9
H−Rh−C−C[c]	87.7	87.3	88	19.7	−19.9	−19.7	89.8	16.8	−24.1
$Rh-H_{hydride}$	1.596	1.596	1.599	1.645	1.645	1.645	1.596	1.641	1.640
C═C	1.403	1.404	1.398	1.411	1.411	1.411	1.407	1.407	1.419
$Rh-C_{alkene}$	2.238	2.238	2.256	2.224	2.223	2.227	2.224	2.237	2.198
$C_{alkene}-H_{hydride}$				1.665	1.668	1.656		1.685	1.658

[a] Energies in kJ·mol^{-1}, distances in Å, and angles in deg. [b] Less stable conformational isomer CCW, which presents a face-to-face stacking interaction instead of a edge-to-face stacking interaction (see text). [c] Dihedral angle $H_{hydride}-Rh-C_{alkene}-C_{alkene}$ for defining alkene rotation.

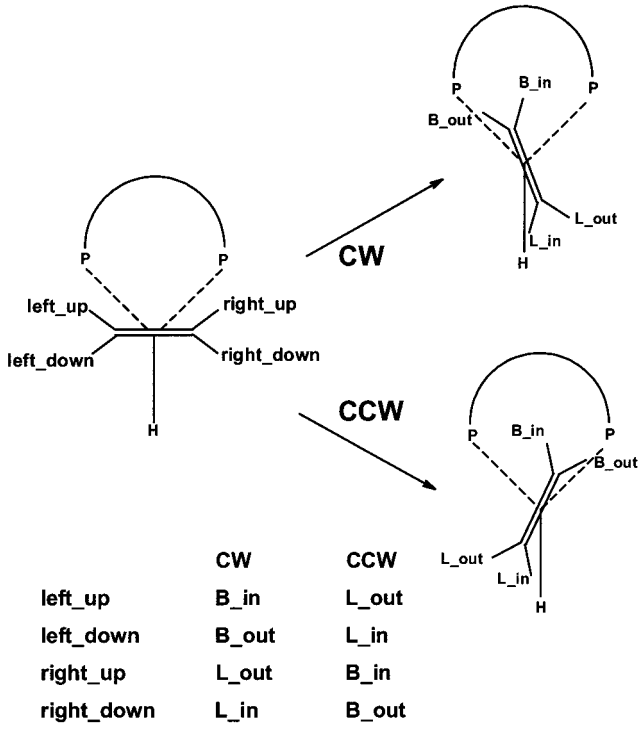

Figure 3. Definition of the eight possible reaction paths for alkene insertion from the key equatorial−equatorial pentacoordinate intermediate.

two transition states for CW and CCW rotations and will be the starting point for the study of substituted alkenes. Table 1 shows the relative energies of the reactant and transition states for both diphosphines as well as some geometric parameters. For each diphosphine, the zero of energy is set to the most stable conformer of **1a**. For benzoxantphos, the computed energy barrier reaches a value of 58 kJ mol^{-1}, the CW and CCW rotations being degenerate. In both TS structures and in contrast to alkene complexes, the edge-to-face stacking interaction is energetically favored, as a pseudosymmetry plane relates the two TS's. For the homoxantphos conformation considered in this work, CW and CCW rotations are not degenerate, the CCW being the most stable one by 7 kJ·mol^{-1} (Table 1). Note that the CW rotation would be the most energetically favored if the other conformation were considered. In the case of benzoxantphos ligand, its conformation can be roughly regarded as pseudo-C_s with respect to the disposition of two diphenylphosphine moieties. On the other hand, the homoxantphos backbone is based on a seven-membered ring instead of a six-membered one and it can adopt two degenerate conformations, which are related by a pseudo-C_2 symmetry operation. Note that diphosphine local symmetry is reflected in the relative stability of the TS. A symmetry plane makes CW and CCW rotations degenerate whereas both rotation sides are energetically different in the case of a C_2 axis. These represent the cases of the two systems considered in this work.

The energy barriers for benzo- and homoxantphos ligands are very similar, and no dramatic changes in the geometrical parameters of reaction centers are observed. However, the computed bite angles are wider in the benzo- than in the homoxantphos system, for both alkene complex and insertion TS structure, which agrees with the previously calculated natural bite angles.[9] Thus, considering the most stable isomers, in alkene complexes the bite angles are 107.4° and 101.8°, whereas in TS's they are 111.4° and 99.9°, for benzo- and homoxantphos, respectively. It is worth mentioning that the calculated energy barriers for the xantphos system are of the same order of magnitude as that previously reported for the insertion process on the related $RhH(CO)_2(PH_3)$ system,[11b,13] in which the computed barrier for the most favorable path was about 90 kJ·mol^{-1}. Also the structures of TS's are closely related for both systems. The ethene ligand has rotated from its equilibrium position on the alkene complex, forming a four-center TS with the hydride ligand bent toward the alkene, whereas the distances of the Rh−H breaking bond and C═C bond are slightly lengthened. Our computed values for the distances of C−H forming bonds in the most stable TS isomers are 1.665 and 1.658 Å, for benzo- and homoxantphos ligands, respectively. These values are comparable to those reported in previous theoretical studies on alkene insertion.[11−13,15] Furthermore, the geometry of the xantphos TS structures shows that the dihedral angle H−Rh−C−C is not zero in any case, which supports the hypothesis that for a substituted alkene there are four possible TS's for each path (CW and CCW), as we have discussed above. For benzoxantphos, since CW and CCW paths are degenerate, only one path must be studied, i.e., four TS's must be characterized. For homoxantphos, eight TS's will play a role, but since CW is energetically less favored, the four TS's arising from the CCW path are expected to be the lower ones. However, we will characterize the eight TS's in order to evaluate their contribution to the regioselectivity.

2. Propene Insertion. Tables 2 and 3 collect the relative total energy for all characterized TS's for the two ligands as well as some geometric parameters. The energies are relative to that of the most stable TS for each ligand. The decomposition of the total energy in their contributions (quantum mechanics and molecular mechanics) is also collected in the tables. The geometries of the TS's for propene insertion are closely related to those described for the ethene insertion.

The same pattern in the relative energy distribution of transition states is observed for both ligands. The lowest energy

Table 2. Propene Insertion for the Benzoxantphos System, Energies and Geometrical Parameters of Transition States[a]

	CW			
	L_out	L_in	B_out	B_in
total energy	0.0	1.5	3.7	8.9
MM energy	0.0	−0.2	2.4	0.5
QM energy	0.0	1.8	1.3	8.4
P−Rh−P	111.0	112.0	111.7	112.3
H−Rh−C−C[b]	18.7	13.4	18.3	12.8
$Rh-H_{hydride}$	1.648	1.639	1.649	1.639
C═C	1.415	1.408	1.413	1.410
$Rh-C_{alkene}$	2.218	2.241	2.264	2.268
$C_{alkene}-H_{hydride}$	1.662	1.688	1.619	1.667

[a] Energies in kJ·mol^{-1}, distances in Å, and angles in deg. [b] Dihedral angle $H_{hydride}-Rh-C_{alkene}-C_{alkene}$ for defining alkene rotation.

transition state is the pro-linear out (L_out) isomer, and the highest energy one is the pro-branched in (B_in). The relative energies of the B_in isomer are 8.9 and 7.8 kJ·mol^{-1} for the benzo- and homoxantphos systems, respectively. Note that the energies of transition states for CW rotation of the homoxantphos system also follow the same trend, but their energies are shifted to higher values due to the increase of MM energy contribution. This increase is associated with the nonbonding repulsive interactions between the alkene substituent and the phenylphosphino substituents, which are well reproduced by the MM method. Despite the many efforts made, in the case of homoxantphos ligand, it has not been possible to find the transition state corresponding to a B_in isomer for CW rotation. However, this isomer is expected to be very high in energy, and consequently it will have little influence in determining the l:b ratio. To confirm this, we carried out additional calculations to estimate the energy of the B_in CW isomer. In all the attempts carried out to obtain B_in CW, the transition state search process ended in the B_out CCW isomer. So, we performed a partial transition state search where the alkene fragment was not allowed to rotate. The results showed that the relative total energy of the B_in CW isomer was around 13.4 kJ·mol^{-1} (the MM energy was around 7.5 kJ·mol^{-1} and the QM energy was around 5.9 kJ·mol^{-1}).

The differences in energy between L_out and B_in isomers are mostly in the QM part. Differences are 8.4 and 9.2 kJ·mol^{-1} for benzo- and homoxantphos, respectively, while differences in MM part are much smaller, 0.5 and −1.4 kJ·mol^{-1} for benzo- and homoxantphos, respectively. Thus, in the context of the IMOMM energy partition scheme and taken into account which atoms are included in each part (QM or MM), a plausible explanation for the energetic differences could come from the reacting centers which are treated quantum mechanically. Analyzing the different TS structures, we observe that in the highest energy isomer (B_in) the methyl alkene substituent is

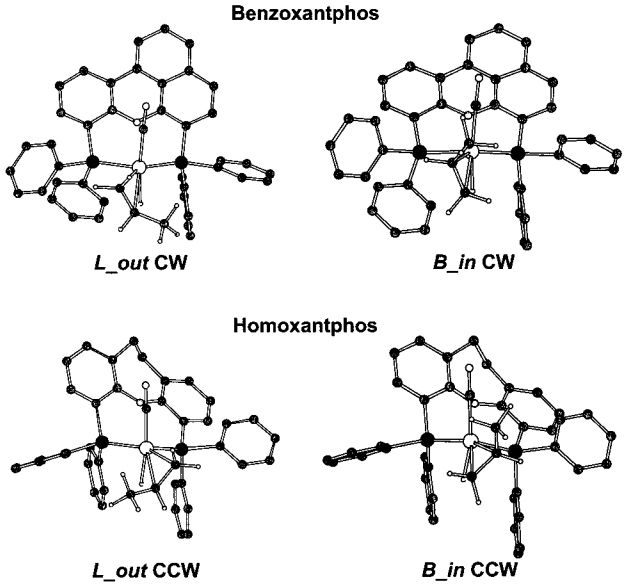

Figure 4. IMOMM TS structures of some representative isomers for propene insertion on benzo- and homoxantphos systems. TS's are presented as in Figure 3 (front view), and the hydrogen atoms of xantphos ligands are omitted for clarity.

parallel to the metal−carbonyl bond, or in other words, that the methyl and carbonyl ligands are eclipsed, a situation that may destabilize the transition state (see Figure 4). Rocha et al.[12] has recently found a similar situation for a model system with PH_3. The difference between pro-linear and pro-branched TS for propene insertion is equivalent in our case since that model system corresponds to our QM part and the difference arises mainly from the double bond polarization and the interaction between the methyl alkene substituent and the CO ligand. If we take a closer look at the geometry of the reaction centers, we cannot observe any clear trend among the series of characterized TS. We have also tried to find some correlation between the relative energies and atomic charges obtained with different partition schemes (Mulliken, NPA), but it has not been possible to find any feature of significant magnitude. Since the extreme energetic cases (L_out and B_in) are similar in both ligand systems, the difference in regioselectivity will be governed by the intermediate cases (L_in and B_out), where a mixture of MM (steric) and QM (electronic) effects is observed.

From the data in Table 2, it is clear that the total energies of CW transition states of the homoxantphos ligand arise mainly from an increase in MM energy contributions. This indicates a steric origin for the energetic differences between the two rotation sides, which could be explained from the structural

Table 3. Propene Insertion for the Homoxantphos System, Energies and Geometrical Parameters of Transition States[a]

	CCW				CW			
	L_out	L_in	B_out	B_in	L_out	L_in	B_out	B_in[b]
total energy	0.0	6.4	2.4	7.8	5.4	6.7	14.7	
MM energy	0.0	2.1	1.1	−1.4	5.1	5.5	11.8	
QM energy	0.0	4.2	1.3	9.2	0.3	1.2	2.9	
P−Rh−P	99.5	99.8	100.6	99.5	100.8	104.3	103.4	
H−Rh−C−C[c]	−21.6	−22.3	−21.5	−25.4	18.3	12.1	17.5	
$Rh-H_{hydride}$	1.643	1.638	1.643	1.633	1.645	1.638	1.648	
C═C	1.420	1.418	1.417	1.425	1.413	1.407	1.412	
$Rh-C_{alkene}$	2.198	2.207	2.240	2.213	2.220	2.250	2.267	
$C_{alkene}-H_{hydride}$	1.673	1.673	1.633	1.646	1.681	1.672	1.611	

[a] Energies in kJ·mol^{-1}, distances in Å, and angles in deg. [b] The CW B_in isomer could not be localized (see text). [c] Dihedral angle $H_{hydride}-Rh-C_{alkene}-C_{alkene}$ for defining alkene rotation.

Table 4. Propene Insertion for the Benzoxantphos−PH_2 System, Energies and Geometrical Parameters of Transition States[a]

	CW			
	L_out	L_in	B_out	B_in[b]
total energy	0.0	1.2	1.8	
MM energy	0.0	−0.4	0.1	
QM energy	0.0	1.6	1.7	
P−Rh−P	118.8	120.2	118.6	
H−Rh−C−C[c]	13.3	4.1	14.7	
$Rh-H_{hydride}$	1.656	1.657	1.653	
C═C	1.413	1.410	1.412	
$Rh-C_{alkene}$	2.236	2.249	2.262	
$C_{alkene}-H_{hydride}$	1.627	1.610	1.617	

[a] Energies in kJ·mol^{-1}, distances in Å, and angles in deg. [b] The CW B_in isomer could not be localized (see text). [c] Dihedral angle $H_{hydride}$−Rh−C_{alkene}−C_{alkene} for defining alkene rotation.

features of the homoxantphos ligand. The backbone induces a different conformation of the two diphenylphosphine moieties, bringing one of them closer to the metal center and increasing the destabilizing nonbonding interactions with the substrate. In this case, the backbone brings the metal center closer to the diphenylphosphine moiety on the right-hand side (front view), which corresponds to CW rotation, the energetically disfavored one. Also, the differences in calculated natural bite angles for transition states of the two rotation sides of the homoxantphos system are worth mentioning. For CCW rotation bite angles range from 99.5° to 100.6°, while for the higher energetic CW rotation calculated bite angles are larger, ranging from 100.8° to 104.3°. These results are in line with the arguments previously reported,[9] in which it is suggested that an increase of steric congestion around the metal center is directly related with larger bite angles. Another feature that can be observed from data in Tables 2 and 3 is that B_out isomers, in both ligand systems, have higher MM energies than their corresponding B_in isomers. If one remembers the labels used to classify transitions states, the "out" notation was used to designate those isomers with the alkene substituent pointing toward the phenyl moieties, away of the CO−Rh−H axis. Thus, it can be derived that in "out" transition states a destabilizing interaction takes place between the aliphatic substituent and the phenyl moieties, which is reflected in an increase of MM energy.

From the initial analysis of energetic results, it can be concluded that, for both ligands, linear product will be obtained predominantly, which is in full agreement with experimental data. The calculated percentages for propene of linear product over branched are 83% for the benzoxantphos and 73% for the homoxantphos system, in good agreement with the reported experimental percentages for 1-octene, 98.1% and 89.5% for the benzoxantphos and homoxantphos systems, respectively. Despite the small differences in regioselectivities exhibited by the two xantphos systems, we succeeded in reproducing the trend. It is also worth mentioning that the alkene used in our calculations is propene instead of 1-octene, a factor that may explain the lower predicted selectivity for linear product. These results are a remarkable success of the IMOMM method and prove its potential application to homogeneous catalysis as a prediction tool in ligand design.

We do not notice any relevant difference in the geometries of the reaction centers between transition states of the two ligand systems, but different ranges in bite angle are observed for the two systems, ranging from 111.0° to 112.3° for benzoxantphos and from 99.5° to 104.3° for homoxantphos. Thus, the more selective diphosphine, benzoxantphos, presents a range of larger bite angles than the less selective homoxantphos. The increase of regioselectivity for linear aldehyde with increasing natural bite angle observed experimentally is well reproduced. Moreover, we prove that the correlation between the bite angle and regioselectivity also takes place at the point where the regioselectivity is decided, i.e., the transition state for alkene insertion, and we can exclude the alkene coordination step as a key step in determining regioselectivity.

3. Analysis of Substrate−Ligand Interactions. To analyze in detail the specific role played by the bite angle and the phenyl substituents of the diphosphine, we determined the regioselectivity that could be afforded by a model system, replacing each phenyl substituent by hydrogen and maintaining the backbone of diphosphine ligands (PH_2 model). Removing the phenyl substituents allows one to put aside the *nonbonding effects* of the phenyls on regioselectivity. Thus, by comparing this result with the regioselectivity computed for the diphenylphosphine catalyst, we were able to evaluate the importance of the interactions between the phenyl substituents and the substrate. Notice that within the IMOMM partition scheme, the phenyl groups are included in the MM part. In this particular case, this scheme allows us to separate, identify, and evaluate the different contributions of the xantphos ligands to regioselectivity. Maintaining benzoxantphos and homoxantphos backbones ensures that the transition states of the PH_2 model system will have different bite angle values for both types of ligands. Thus, once the phenyls have been removed, and by comparison between both types of ligands, we may obtain an evaluation of the effect directly associated to the bite angle (*orbital effect*) on regioselectivity. It is worth mentioning that some preference for linear or branched products is expected due to the intrinsic regioselectivity of the substrate, as we have already seen above.

Tables 4 and 5 collect the results for these PH_2 model systems. As in the diphenylphosphine system, a different range of bite angle values for the two types of ligands is observed in the model system. The bite angles for the transition states with

Table 5. Propene Insertion for the Homoxantphos−PH_2 System, Energies and Geometrical Parameters of Transition States[a]

	CCW				CW			
	L_out	L_in	B_out	B_in	L_out	L_in	B_out	B_in[b]
total energy	0	2.9	0.9	8.1	−0.1	1.7	0.2	
MM energy	0	0.4	0.2	0.2	−0.2	0.4	−0.6	
QM energy	0	2.5	0.8	8.0	0.1	1.3	0.8	
P−Rh−P	101.7	103.7	102.4	102.9	101.2	104.9	101.6	
H−Rh−C−C[c]	−20.2	−14.5	−24.5	−16.9	20.6	12.7	22.5	
$Rh-H_{hydride}$	1.643	1.635	1.643	1.633	1.643	1.634	1.641	
C═C	1.418	1.410	1.418	1.415	1.414	1.406	1.415	
$Rh-C_{alkene}$	2.204	2.228	2.229	2.249	2.210	2.239	2.235	
$C_{alkene}-H_{hydride}$	1.673	1.703	1.641	1.674	1.702	1.724	1.666	

[a] Energies in kJ·mol^{-1}, distances in Å, and angles in deg. [b] The CWB_in isomer could not be localized (see text). [c] Dihedral angle $H_{hydride}$−Rh−C_{alkene}−C_{alkene} for defining alkene rotation.

Table 6. Calculated vs Experimental Regioselectivities

			calculated (propene)			
	exptl (1-octene)		diphenylphosphine model		PH_2 model	
ligand	βn[a]	% l over b[b] (l:b ratio)	P−Rh−P[c]	% l over b[d] (l:b ratio)	P−Rh−P[c]	% l over b[d] (l:b ratio)
benzoxantphos	120.6	98.1 (50.2)	111.0−112.3	83 (4.9)	118.8−120.2	74 (2.7)
homoxantphos	102.0	89.5 (8.5)	99.5−104.3	73 (2.8)	101.2−104.9	63 (1.7)

[a] Calculated natural bite angle (βn) in degrees (cf. ref 9). [b] Experimental regiolectivities (linear over branched percent and ratio) for hydroformylation of 1-octene (cf. ref 9). [c] Range of calculated bite angles of the transition states for propene insertion. [d] Calculated regioselectivities (linear over branched percent and ratio) from relative energies of transition states for propene insertion.

benzoxantphos range from 118.8° to 120.2° whereas for homoxantphos the values are between 101.2° and 104.9°. Moreover, larger bite angles were observed in the PH_2 model system than in the diphenylphosphine system for both ligands. The bite angle of benzoxantphos complexes increases over 7° while in homoxantphos it increases less than 2°. This effect is mainly due to the loss of nonbonding interactions, i.e., the stacking between the two phenyls in the backside of the xantphos backbone and the interactions between the ligand and the substrate.

Table 6 shows a comparison between the experimentally observed regioselectivity and predicted regioselectivities for the PH_2 and diphenylphosphine model systems. Predicted regioselectivities in the PH_2 model system for linear product over branched are 74% for benzoxantphos and 63% for homoxantphos. From diphenylphosphine to PH_2, regioselectivities are substantially reduced for both ligands (from 83% to 73% and from 74% to 63%, respectively). For the PH_2 model system, a difference between benzoxantphos and homoxantphos is still observed; however, this difference has become proportionally less important. If percentages are translated into l:b ratio, we realize that the difference in l:b ratio for the diphenylphosphine system is 2.2 (4.9 and 2.7 for benzo- and homoxantphos, respectively) while the difference for the PH_2 model system is only 1.1 (l:b ratio is 2.8 and 1.7 for benzoxantphos and homoxantphos in the model system, respectively).

From Tables 4 and 5, it is clear that most of the energy differences between the different TS's are in the QM part, with the MM part being nearly the same. This clearly proves that when phenyls are removed the regioselectivity is not governed by the nonbonding interactions between the diphosphine and the substrate. So, it seems that the leading role in determining the regioselectivity is played by the phenyl diphosphine substituents. The effect arising from the bite angle, i.e., the *orbital effect*, seems to have little influence on determining regioselectivity, since the difference on selectivities for both ligands in the PH_2 model system is proportionally small compared to those observed in the diphenylphosphine system. This conclusion cannot be extrapolated to other reactions, since for palladium−diphosphine RCN reductive elimination a clear orbital effect on the reaction rate had been observed.[34] Nevertheless, the correlation found experimentally between the bite angle and the regioselectivities had suggested that the bite angle plays an important role in determining regioselectivity. However, this effect has been transferred from the bite angle induced by the ligand backbone to the nonbonding interactions between the phenyls and substrate. Wider bite angles increase the steric interaction of diphosphine substituents with branched species, which become more destabilized. Thus, it is expected that the use of groups bulkier than phenyl groups will lead to higher l:b ratios.

(34) Marcone, J. E.; Moloy, K. G. *J. Am. Chem. Soc.* **1998**, *120*, 8527.

Concluding Remarks

For the first time, Rh−diphosphine catalyzed hydroformilation has been studied by an integrated molecular orbital/molecular mechanics method, IMOMM. We have shown that this method is able to reproduce the observed experimental trends in regioselectivity, by considering the relative stability of all possible transition states. We have proved that correlation between natural bite angles and regioselectivity takes place at the point where the regioselectivity is determined: the transition states for alkene insertion. The IMOMM energy partition scheme allowed the identification and quantification of the nonbonding and the orbital effects. The leading role in determining the regioselectivity is played by the diphenylphosphino substituents. When the steric effects of the phenyls are removed, an important decrease in regioselectivity is observed although all TS structures have larger bite angles. The *orbital effect* seems to have little influence in determining regioselectivity, since the differences in selectivities for both ligands in the model system are proportionally smaller than those observed in the diphenylphosphine system. And finally, our computational model has been able to go one step further in unraveling the complex web of steric effects that governs regioselectivity.

Acknowledgment. Financial support from the Spanish DGICYT under Projects PB98-0916-C02-01 and PB98-0916-C02-02 and from the CIRIT of the Generalitat de Catalunya under Projects SGR-1999-00089 and SGR-1999-00182 is gratefully acknowledged. F.M. thanks DURSI. We thank José C. Ortiz for his technical expertise.

Supporting Information Available: Tables of energies and Cartesian coordinates (PDF). This material is available free of charge via the Internet at http://pubs.acs.org.

JA0101678